Laser excitation spectroscopy of the *A* and *B* states of jet-cooled copper dimer: Evidence for large electronic isotope shifts

John G. McCaffrey,[a] Robert R. Bennett, Michael D. Morse, and W. H. Breckenridge[b]
Department of Chemistry, University of Utah, Salt Lake City, Utah 84112

(Received 21 December 1988; accepted 23 March 1989)

Fluorescence excitation spectra recorded for the *A*–*X* system of jet-cooled Cu_2 show conclusive evidence of a $\Delta\Lambda = 0$ transition, and the *A* state is thereby definitively assigned as $^1\Sigma_u^+$. A previous assignment of the *B* state as $^1\Sigma_u^+$ is confirmed, but the vibrational levels of this state are complicated by the presence of a perturbation at $v' = 0$. The perturbing state does not, however, appear to be either of the two optically accessible electronic states in this spectral region. Anomalously large electronic isotope shifts are observed for the *A* and *B* states, and this behavior is discussed in terms of the correspondingly large "specific mass shifts" observed in the optical spectra of atomic copper for transitions that couple states differing in the number of *d* electrons. Due to the large spin-orbit coupling constants in the "*d*-hole" configurations, it is proposed that the low-energy-excited molecular states of Cu_2 derived from these configurations should be described by Hund's case (c) coupling. Dynamical effects observed in the gas phase and in solid matrices are briefly discussed in terms of this bonding scheme.

I. INTRODUCTION

Knowledge of the electronic characteristics of species involved in a chemical reaction, whether it be in the form of a full collision or half collision encounter, is essential in providing an understanding of such a process.[1] The electronic characteristics of atomic systems are extensively documented[2] and well understood,[3] but until recently virtually no information existed for nonhydride molecular systems involving *d* or *f* group metal atoms.[4] Copper dimer, however, is a transition metal diatomic molecule that has been studied in detail for several years, and for which spectroscopic constants and state assignments exist.[5] With the availability of molecular constants for the low-lying electronic levels of Cu_2, these states are appropriate selections for use in state-specific investigations of intermolecular chemical reaction dynamics. However, when spectra corresponding to transitions from the ground state to the *A* and *B* states of Cu_2 were recorded in the present study, previously unreported behavior was observed in both systems, and a vibrational perturbation was observed in the *B* state.

The spectroscopy of multimer species and, in particular, metal clusters, has in recent years seen considerable advances.[5] This has arisen in large part from the combined use of two diverse experimental techniques. First, the laser vaporization technique allows for the generation of vapors of virtually any elemental or mixed elemental species.[6] Second, the attainment of very low temperatures without bulk condensation using supersonic gas beams yields considerable spectroscopic simplification and enables the spectroscopist to extract information from what would otherwise be very congested spectra.[7] The use of resonant two-photon ionization spectroscopy (R2PI) has been exploited extensively and contributed greatly in such studies by providing laser excitation spectra of mass-selected species. In the present study of Cu_2, laser-induced fluorescence excitation spectra have been obtained for the first few vibrational bands in the *A*–*X* and *B*–*X* systems, providing a definitive state assignment for the *A* state and a confirmation of a previous assignment for the *B* state. More importantly, however, this study has identified significant electronic isotope shifts in both the *A* and *B* molecular states of copper dimer. These small but significant shifts might not be noticed in mass-resolved excitation spectra unless particular attention was paid to small deviations in experimental and calculated line positions between spectra of mass-selected isotopic species.

Since the copper dimer literature has been thoroughly reviewed recently by Morse,[5] only those aspects pertaining directly to the *A*–*X* and *B*–*X* systems will be discussed. From a study of isotope shifts on red-degraded bands present in the blue and green spectral regions, Kleman and Lindkvist[8] identified the source of the emissions as copper dimer and established absolute vibrational numbering. Vibrational constants for the *X*, *A*, and *B* states were calculated from bandhead positions. Rotationally resolved spectra recorded by Åslund *et al.*[9] for the 1–0 and 0–0 bands of the *B*–*X* system identified the transition as $^1\Sigma_u^+ - {}^1\Sigma_g^+$ and yielded equilibrium internuclear separations of 2.3274 and 2.2195 Å for the excited and ground states, respectively. The value of ω_o' for the *B* state was determined by these workers to be 242.15 cm^{-1} from measurements of band origins. This value is in approximate agreement with the corresponding value measured by Kleman and Lindkvist[8] but deviates significantly from the value obtained by fitting other vibrational bands with constants derived by the latter workers.

Pesič and Weniger[10] identified apparent *Q* branches in the *A*–*X* system and thereby assigned the *A* state as $^1\Pi_u$. Subsequent work by Lochet[11] on this system identified only *P* and *R* branches, and the *A* state was accordingly assigned

[a] Present address: Institute für Atom- und Festkörperphysik, Freie Universität Berlin, Arnimallee 14, D-1000 Berlin 33, West Germany.
[b] Author to whom correspondence should be addressed.

 0021-9606/89/130092-12$02.10

as $^1\Sigma_u^+$. Gole and co-workers[12] reported spectra obtained by laser-induced fluorescence spectroscopy in a supersonic expansion of pure copper vapor for the *B–X* system. Although spectral simulations were presented in this study, spectroscopic constants were not reevaluated for the *X* or *B* states. Using laser vaporization to generate an effusive source of copper vapor entrained in cooled helium carrier gas, Bondybey and co-workers[13] obtained laser-induced fluorescence excitation spectra of the *A–X* and *B–X* systems. Radiative lifetime measurements indicated significant nonradiative decay channels for both states. Collision-free radiative lifetimes of $v = 0$ in the *A* state were found to be 115 ± 10 ns, with indications of efficient predissociation processes occurring in this electronic state. Population cascading from a high energy *B'* state (labeled *C* by other workers, see Ref. 5) render extraction of intrinsic radiative lifetimes for the *B* state somewhat uncertain, but the collision-free value reported is 40 ± 5 ns. By dispersing the fluorescence resulting from near-UV laser excitation of the Cu_2 *II–X* absorption system in a supersonic expansion, Rohlfing and Valentini[14] obtained accurate vibrational constants for the ground state.

Matrix-isolation studies of the *A* and *B* states of copper dimer have been reported by Bondybey and co-workers[15,16] using neon as the host solid. Laser excitation spectra of the *A* and *B* states indicated structureless profiles and vibrationally relaxed emission for both electronic states. Dispersion of the resulting emission revealed structured profiles whose splittings corresponded to the ground-state vibrational frequencies. By identifying the $a\ ^3\Sigma_u^+ - X\ ^1\Sigma_g^+$ system of Cu_2, this matrix study[17] demonstrated very nicely the manner in which the properties of the solid state can be used to provide population in levels inaccessible by optical techniques. More recently Wiggenhauser *et al.*[18] measured the radiative lifetime of the *B–X* system in solid matrices and observed double exponential decay, with time constants of 9.8 and 11.5 ns.

Several theoretical approaches have been utilized in the study of ground-state copper dimer.[5] Incorporation of correlation[19] and relativistic effects,[20] however, appears to be essential in obtaining molecular parameters consistent with the well-established ground-state spectroscopic constants. Few high level *ab initio* studies appear to exist for excited molecular states of Cu_2 derived from asymptotes other than $^2S + {}^2S$, and one calculation by Witko and Beckmann[21], which includes $^2S + {}^2D$ asymptotes, is restricted to a description of molecular states in terms of Hund's case (a).

This paper is structured as follows: In Sec. II a brief description of the experimental apparatus used in obtaining laser-induced fluorescence excitation spectra in an ultracold supersonic jet is presented. The excitation spectra recorded for the *A–X* and *B–X* systems of jet-cooled copper dimer are presented in Sec. III, along with an analysis of the vibrational structure of the $B\ ^1\Sigma_u^+$ state. Section IV provides a detailed outline of the spectral simulation procedures. Discussion of the fits between experimental and simulated spectra is presented in Sec. V A, and the need for including an electronic isotope shift in both the *A–X* and *B–X* transitions is demonstrated. Possible origins of this electronic isotope shift are considered in Sec. V B in terms of adiabatic corrections, and are shown to be insufficient to account for the magnitude of the observed shifts. The subject of electronic isotope shifts is discussed further in Sec. V C with regard to the large specific mass shifts known to be present in the ^2D_J levels of atomic copper derived from the $3d^9 4s^2$ configuration. Spectra recorded for the $^2P_{1/2}$–$^2D_{3/2}$ transition are presented in this section. From the approximately equal magnitude and sign of the isotope shift observed on this atomic transition and on the *A–X* and *B–X* systems of Cu_2, it is suggested that a correlation may exist between the two effects. This idea is developed in greater detail in Sec. V D, where the possible Hund's coupling cases of the excited states of Cu_2 are presented and critically appraised.

II. EXPERIMENTAL

The apparatus used in the present study was designed specifically for the production of van der Waals' molecules and has been described in detail in an earlier publication.[22] Briefly, the copper dimer was produced by focusing the second harmonic output of a *Q*-switched Molectron model MY-32 Nd:YAG laser onto a 0.25-in.-diam metal target rod. The resulting plasma was entrained in a flow of helium gas by synchronously opening a pulsed valve (General Valve Corporation) having a backing pressure of ~ 4 atm. Adiabatic expansion of the helium/copper vapor mixture into a chamber evacuated by an Edwards EH2600 Roots blower backed by an Edwards E2M175 mechanical pump resulted in the formation of an ultracold gas jet. Detection was achieved using laser-induced fluorescence produced in the supersonic expansion by orthogonally intersecting a dye laser beam approximately 40 nozzle diameters downstream. The timing of the gas pulse, Nd:YAG vaporization laser and the Lumonics, HyperEX-420 XeCl, excimer-pumped dye laser (Lumonics HyperDYE-300) was varied with a BNC model 7010 digital delay generator to optimize the photocurrent output of a Hamamatsu R919 photomultiplier tube used for photon detection. This signal was fed to a PAR boxcar integrator (model 162), the output of which was recorded on an *X–Y* plotter. Interference filters were used to limit the range of detected emission to that appropriate for the $A \rightarrow X$ and $B \rightarrow X$ fluorescence bands. The laser dyes used in these regions were Coumarin 480, Coumarin 460, and Coumarin 440 (Exciton).

All the spectra shown herein were recorded with the maximum detection sensitivity available in the present experimental configuration. This enabled saturation and power-broadening effects to be avoided by attenuating the unfocused output of the Lumonics HyperDYE 300 laser, which was operated as an oscillator without amplification. The laser beam size in the viewing region was ~ 5 mm in diameter and the power density typically $0.1\ \mu J/cm^2$. Spectra of metastable ^2D atomic Cu transitions were recorded with very low vaporization laser (Nd:YAG) power with the lowest laser excitation intensities to avoid any line-broadening effects.

III. RESULTS

A laser-induced fluorescence excitation spectrum recorded for the 0–0 band of the *A–X* system of a jet-cooled copper dimer is shown by trace (a) in Fig. 1. From the par-

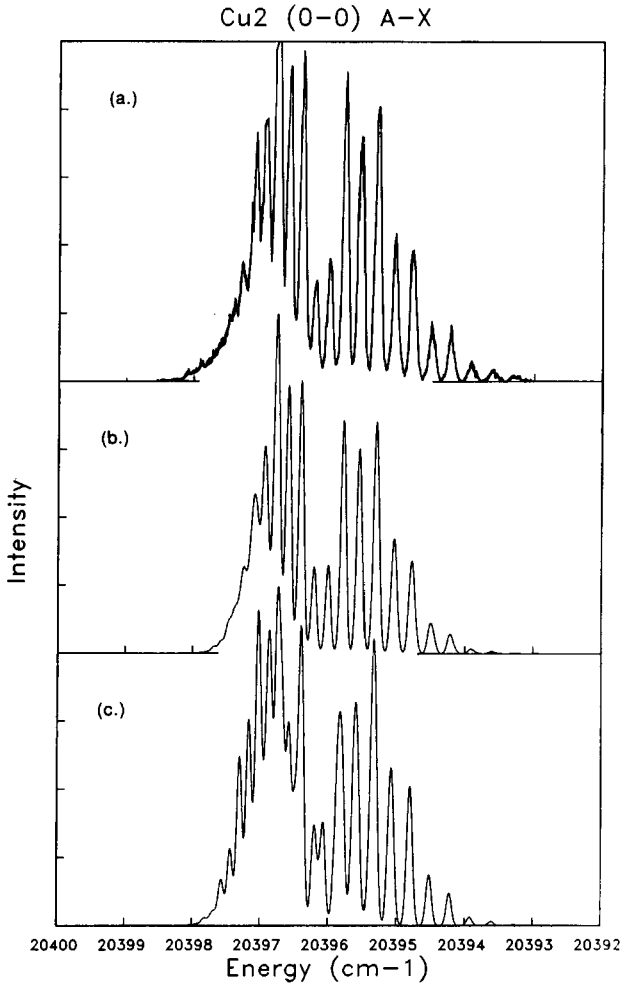

FIG. 1. Laser-induced fluorescence excitation spectrum recorded for the 0–0 band in the *A*–*X* system of a jet-cooled copper dimer is shown by trace (a). Traces (b) and (c) are spectral simulations obtained with the spectroscopic constants listed in rows 2 and 3 of Table III using a rotational temperature of 2.3 K and a laser linewidth (FWHM) of 0.08 cm^{-1}. Electronic isotope shifts of $+0.06$ and $+0.12$ cm^{-1} in the band origins of $^{63}Cu^{65}Cu$ and $^{65}Cu_2$ with respect to $^{63}Cu_2$ were included in the simulation of (b). No such shifts were included in the simulation of (c), where it is obvious that agreement with the experimental spectrum in trace (a) is poor.

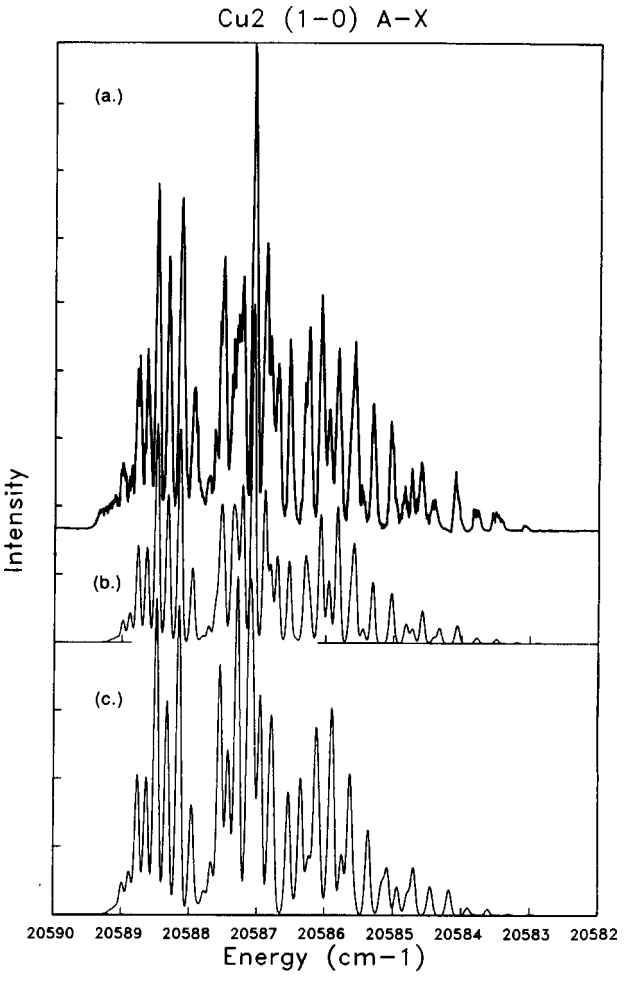

FIG. 2. Laser-induced fluorescence excitation spectra of the *A*–*X* 1–0 band of Cu_2. Spectral simulations were obtained using identical parameters as those used in Fig. 1. The intensity alternation in the completely resolved *R* branch of the $^{63}Cu_2$ homonuclear species is evident on the left of the figure. As in Fig. 1, agreement between simulated and experimental spectra is obtained when an electronic isotope shift is considered [trace (b)].

tially resolved rotational structure present in this spectrum, it is evident that only *P* and *R* branches exist. This pattern is demonstrated more clearly in the 1–0 band shown by trace (a) in Fig. 2, where vibrational isotope shifts result in partially resolved rotational transitions for the three isotopic variants of dimeric copper, viz., 63–63, 63–65, and 65–65, whose relative abundances are 47.73%, 42.71%, and 9.56%, respectively. Without recourse to spectral simulation, the *A*–*X* transition of copper dimer can be ascribed to having $\Delta\Lambda = 0$. Since no *Q*-branch is present, and the ground state is known to be $^1\Sigma_g^+$,[9] the *A* state can be definitively assigned as $^1\Sigma_u^+$.

Experimental spectra recorded for the 0–0 and 1–0 transitions of the *B*–*X* system are shown by traces (a) in Figs. 3 and 4, respectively. As in the *A*–*X* system the absence of a *Q*-branch indicates a Σ–Σ transition. This observation confirms the earlier $^1\Sigma_u^+$ assignment of Åslund *et al.*[9] for the *B* state. In contrast to the agreement concerning state assignment, however, considerable confusion exists in the literature regarding the vibrational constants of this state.[5] We have recorded rotationally resolved spectra for the vibrational bands accessible by Franck–Condon transitions from the $v'' = 0$ level of jet-cooled Cu_2. The positions of the $^{63}Cu_2$ $P(1)$ rotational lines were observed to be 21 747.66, 21 989.61, 22 226.83, 22 460.06, 22 689.39, 22 914.45, and 23 135.82 cm^{-1} for the bands in the range $v' = 0$ to $v' = 6$, respectively. Identification of the $P(1)$ line is rather straightforward in the *B*–*X* system because of the spectroscopic simplicity of this $^1\Sigma$–$^1\Sigma$ transition and is a convenient choice in evaluating accurate vibrational constants since it has a constant red shift of $2B_0''$ from the band origin for all the $v'' = 0$ transitions of jet-cooled Cu_2. A Birge–Sponer plot of $\Delta G'_{(v+1/2)}$ derived from the observed $P(1)$ line positions, for the vibrational bands in the range $v' = 0$ to $v' = 6$, was linear with the exception of the first interval. The vibrational constants $\omega_e', \omega_e'x_e'$ were found to have values of 245.7 ± 0.3, and 2.05 ± 0.03 cm^{-1}, and 245.2 ± 0.15 and 2.00 ± 0.01 cm^{-1}, respectively, depending on whether the observed value of ν_{00} was considered or ignored in the least-squares fit (listed uncertainties represent $\pm 1\sigma$). A possible perturbation in this level is discussed in Sec. V A.

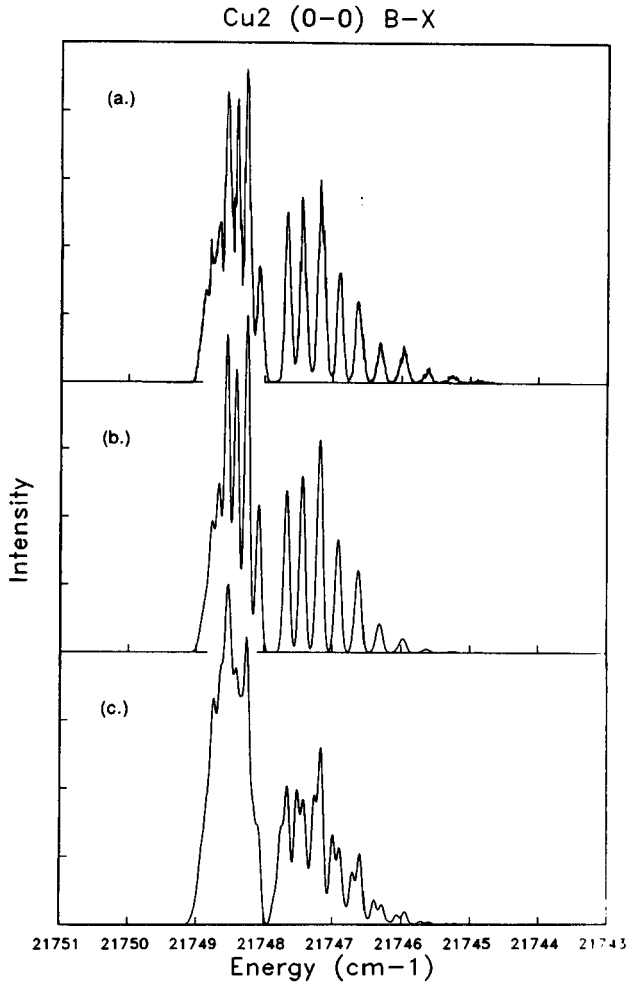

FIG. 3. *B–X* 0–0 LIF excitation spectrum of jet-cooled copper dimer. Spectral simulations (b) and (c) were obtained using the spectroscopic constants listed in rows 1 and 3 of Table III. A rotational temperature of 2.00 K and a laser linewidth of 0.08 cm^{-1} was used in generating both simulations. Trace (b) includes electronic isotope shifts of + 0.06 and + 0.12 cm^{-1} in the band origin positions of $^{63}Cu^{65}Cu$ and $^{65}Cu_2$ with respect to $^{63}Cu_2$.

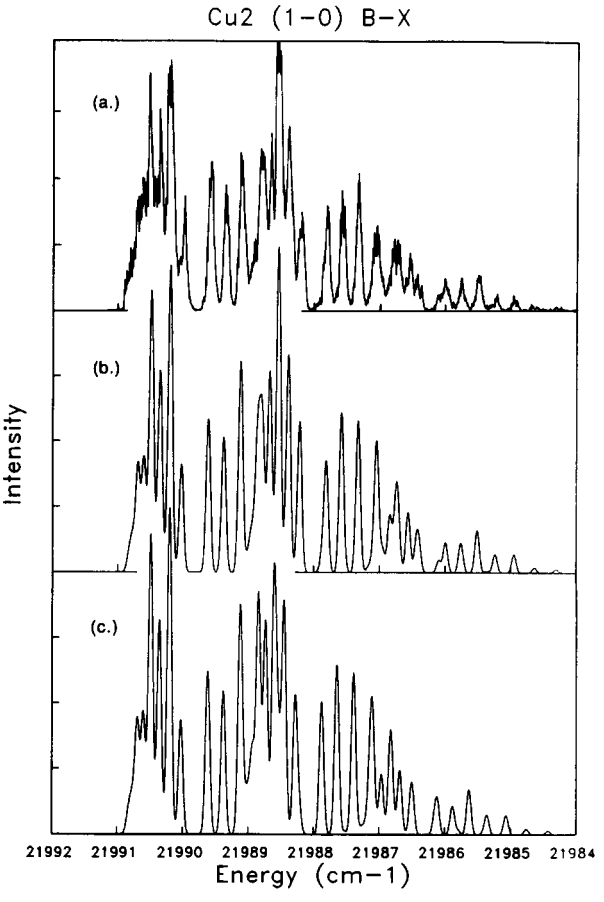

FIG. 4. Spectral simulations of the 1–0 band of the copper dimer *B–X* system. Traces (b) and (c) in this figure were obtained with identical parameters as those used in the corresponding simulations in Fig. 3. The isotopic variants of Cu_2 can be identified easily in this spectrum because of the vibrational isotope shift in the band origins. An intensity alternation in the resolved lines in the *R* and *P* branches on the left of this figure indicate $^{63}Cu_2$, while the absence of such alternation in the corresponding branches in the central portion of the spectrum is due to $^{65}Cu^{63}Cu$. The low natural abundance of the $^{65}Cu_2$ species makes its identification on the extreme right of the figure less obvious.

To extract spectroscopic constants from the recorded spectra, shown by trace (a) in Figs. 1–4, spectral simulations were performed on transitions to the low vibrational levels in the electronically excited *A* and *B* states. It became evident in the simulation procedure, however, that while the reported *A* state spectroscopic constants yielded satisfactory fits to the experimental spectra in isotopically resolved regions of $v' > 0$ bands, poor fits were obtained for the 0–0 vibrationless transition. Careful reexamination of the relative rotational line positions between the three isotopic variants of copper dimer indicated systematic deviations from the positions predicted with an assumed electronic isotope shift of zero, even in the $v' > 0$ levels. Because of this rather unexpected finding of a significant electronic isotope shift in a moderately heavy diatomic species such as copper dimer, the simulation procedure is outlined in detail below.

IV. SIMULATION

The rotational line positions in the *P* and *R* branches of a $^1\Sigma$–$^1\Sigma$ transition centered about a band origin ν_0 are, for a single isotopic combination, given by the standard expressions[23]:

$$\nu_P(J) = \nu_0 - (B'_v + B''_v)J + (B'_v - B''_v)J^2, \quad (1)$$

$$\nu_R(J) = \nu_0 + 2B'_v + (3B'_v - B''_v)J + (B'_v - B''_v)J^2, \quad (2)$$

respectively. Single and double prime symbols represent excited and ground-state qantities, respectively, while the running subscript v for the rotational constant B denotes the variation of the rotational constant with vibrational level. B_v is calculated as

$$B_v = B_e - \alpha_e(v + 1/2), \quad (3)$$

where α_e is the vibration–rotation interaction constant. Variation in the magnitude of the rotational constants B_e and α_e with isotopic substitution is given by the relations[23]

$$B^i_e = \rho_i^2 \cdot B_e \text{ and } \alpha^i_e = \rho_i^3 \cdot \alpha_e, \quad (4)$$

where ρ_i is defined as $(\mu/\mu_i)^{1/2}$, and μ and μ_i represent the reduced masses of the lighter ($^{63}Cu_2$) and heavier ($^{63}Cu^{65}Cu$ or $^{65}Cu_2$) isotopic combinations, respectively.

The variation of the vibrational band origins with isotopic substitution is[23]

$$\Delta = \nu - \nu_i = (1-\rho_i)\left[\omega_e'(v'+\tfrac{1}{2}) - \omega_e''/2\right] - (1-\rho_i^2)\left[\omega_e'x_e'(v'+\tfrac{1}{2})^2 - \omega_e''x_e''/4\right] + (1-\rho_i^3)\left[\omega_e'y_e'(v'+\tfrac{1}{2})^3 - \omega_e''y_e''/8\right], \quad (5)$$

for transitions involving the vibrationless level in the ground state. Truncation of the series at the $(1-\rho^2)$ term is accurate, as in the present study, for the lowest vibrational levels in the excited state. For the 0–0 band it is apparent from Eq. (5) that the isotopic shift in the band origins depends largely on the difference in the upper and lower electronic state equilibrium vibrational frequencies. Using the $^{63}Cu_2$ 0–0 transition frequency ν_{00}, the band origins of higher vibrational levels can be obtained from the following relationship

$$\nu_{v',v''} = \nu_{00} + \omega_e'v' - \omega_e'x_e'(v'^2+v') + \omega_e'y_e'(v'^3+3/2v'^2+3/4v') - \left[\omega_e''v'' - \omega_e''x_e''(v''^2+v'') + \omega_e''y_e''(v''^3+3/2v''^2+3/4v'')\right]. \quad (6)$$

For transitions involving the ground-state $v''=0$ this simplifies to

$$\nu_{v',0} = \nu_{00} + \omega_e'v' - \omega_e'x_e'(v'^2+v') + \omega_e'y_e'(v'^3+3/2v'^2+3/4v'). \quad (7)$$

Isotopic variation in the band origins of excited vibrational levels is calculated using Eq. (5).

Assuming an emission signal linear with laser excitation intensity the Hönl–London factors for a $^1\Sigma$–$^1\Sigma$ transition are given by J and $J+1$ for the P and R branches, respectively, where J pertains (in absorption or excitation) to the ground-state rotational quantum number. The population distribution over ground-state rotational levels is assumed to follow Boltzmann statistics and is given by

$$\frac{1}{Q_r^i}\left\{\exp\left[-J(J+1)\cdot\frac{B_0^i hc}{kT}\right]\right\}.$$

To allow for correct variation of the population in the rotational levels between the isotopic variants, the exponential term includes the appropriate rotational constant B_0^i for each combination. The rotational partition function Q_r^i is also isotope dependent and is evaluated as a sum rather than as an integral since the effective rotational temperature was low ($\sim$2 K). As shown in Table I atomic copper consists of two naturally occurring isotopes, 63 and 65, both having nuclear spin of $I=3/2$. The resulting intensity alternation between even and odd rotational levels in the homonuclear combinations of copper dimer is 3 to 5. The abundance of the three isotopic variants of copper dimer is given in Table II. Finally, the simulated spectra are generated by convoluting the calculated line position/intensities with a Gaussian line shape function describing the finite bandwidth of the scanning dye laser. No account is taken of the Doppler linewidth in the jet, which under the current experimental conditions is at least 2 orders of magnitude less than the bandwidth of the laser.

TABLE I. Properties of the two isotopes of atomic copper.

	^{63}Cu	^{65}Cu
Mass[a]	62.929 599	64.927 792
% Abund[b]	69.09	30.91
I ($\hbar$)[c]	3/2	3/2
μ (nm)[d]	+2.222 8	+2.381 2
Q (b)[e]	−0.211	−0.195

[a] A. H. Wapstra and K. Bos, At. Data Nucl. Data Tables **19**, 177 (1977).
[b] G. H. Fuller and A. O. Nier, Table 8b-1, in *American Institute of Physics Handbook*, 3rd ed. (McGraw-Hill, New York, 1972).
[c] G. H. Fuller, J. Phys. Chem. Ref. Data **5**, 835 (1976).
[d] μ is the nuclear magnetic dipole moment in units of the nuclear magneton (nm).
[e] The nuclear quadrupole moment Q is quoted in barn units (b).

The value of the laser linewidth was obtained by examining the experimental bandwidth for the rotationally resolved transition in the v'–0″ bands of each system. i.e., where $v'>0$. The bandwidth was found to be 0.08 cm^{-1} for the (1,0) and (2,0) vibrational bands of each system, and invariant among the resolved rotational transitions. As a result, it would appear that the only remaining (and usually very small) splitting that can exist for this nondegenerate spin and orbital molecular state, the electric quadrupole fine structure, is much smaller than the laser linewidth.

V. DISCUSSION

A. Fits to data

The spectroscopic constants found to give the best agreement between simulated and recorded spectra are collected in Table III. All the entries in this table correspond to those given in the recent review by Morse,[5] with the exception of the B-state vibrational constants. The values of ω_e',$\omega_e'x_e'$, and $\omega_e'y_e'$ observed in the present rotationally resolved study of the B–X system are 245.20, 2.00, and +0.0003 cm^{-1}, respectively. These values were obtained by fitting the observed $P(1)$ lines to the polynomial expression of Eq. (7) and are in approximate agreement with the corresponding values of 245.8, 2.00, and −0.02 cm^{-1} obtained by Kleman and Lindkvist[8] from a study of bandhead positions. It must, however, be remarked that the observed $P(1)$ line position of the 0–0 band was not included in the fit, as mentioned in Sec. III above. It appears likely that this vibrational level is perturbed. However, from a consideration of perturbation selection rules,[24] and the energies of the optically accessible A and C^5 states of Cu_2, it is concluded that perturbational coupling must be occurring to a dark state.

TABLE II. Mass data of the isotopes of Cu_2 used in the calculation of the line positions.

	$^{63}Cu_2$	$^{63,65}Cu_2$	$^{65}Cu_2$
μ	31.464 799 6	31.956 540 8	32.463 896 2
ρ[a]	1	0.992 276 266	0.984 491 939
% Abund.	47.73	42.71	9.56

[a] ρ is defined as $[\mu(^{63}Cu_2)/\mu_i]^{1/2}$.

TABLE III. Spectroscopic constants (in cm^{-1}) of the *X*, *A*, and *B* states of $^{63}Cu_2$.

State	ν_{00}	ω_e	$\omega_e x_e$	$\omega_e y_e$	B_e	α_e
$B\,^1\Sigma_u^{+a}$	21 747.88	245.20	2.00	+0.0003	0.098 89	0.000 606
$A\,^1\Sigma_u^{+b}$	20 396.00	192.47	0.353	−0.0186	0.102 76	0.000 917
$X\,^1\Sigma_g^{+c}$	0.00	266.43	1.035	+0.0017	0.108 74	0.000 614

[a] *B* state rotational constants are those of Åslund *et al.*, Ref. 9, while the vibrational constants were obtained in the present study. The quoted value of $\nu_{00} = 21\,747.88\ cm^{-1}$ is the experimentally observed value. By a polynomial fit of the band origins in the range $v' = 1$ to 6 to Eq. (7), the value of ν_{00} is predicted to be $0.75\ cm^{-1}$ higher than the observed value. See text for details.

[b] Constants from Lochet, Ref. 11.

[c] Rotational constants of the *X* state are those quoted by Åslund *et al.*, in Ref. 9 while the vibrational constants are taken from the work of Rohlfing and Valentini, Ref. 14.

A comparison of the experimental data and spectra simulated using the spectroscopic constants of Table III is shown in traces (a) and (c), respectively, of Figs. 1–4. It is obvious that poor agreement is obtained, particularly in Figs. 1 and 3, where 0–0 bands of the *A*–*X* and *B*–*X* systems are shown. Note, however, that in regions of the excitation spectra where the rotational structure is resolved, such as in Figs. 2 and 4, excellent agreement exists between simulated and experimental spectra for a given isotope. We conclude that the rotational constants and the expressions relating their variation between the different isotopic forms are correct. The most obvious factors that could produce the poor agreement between experiment and simulation are (a) the magnitudes of the vibrational constants or (b) the expressions relating their isotopic variation.

Since all the bands observed in the present study involve the $v'' = 0$ ground-state level and low vibrational levels in the *A* and *B* states, the expression [Eq. (5)] relating the vibrational isotope shifts is dominated by the $(1 - \rho)$ term. Thus, the observed discrepancies might appear to originate in the use of an inappropriate value for the difference in the excited and ground-state vibrational frequencies. It is clear, however, that such is not the case because adjusting this difference (i.e., $\omega_e' - \omega_e''$) to yield a fit in the 0–0 band results in nonsensical shifts for levels other than $v' = 0$.

Table IV lists the observed and calculated line positions of the three isotopic variants of Cu_2 in the 2–0 band of the *A*–*X* system. It is evident from the differences between calculated and experimental peak positions that systematic deviations exist for the 63–65 and 65–65 species. The average deviation is $+0.05 \pm 0.01\ cm^{-1}$ for the former and $+0.08 \pm 0.02\ cm^{-1}$ for the latter. Deviations of similar magnitude were observed for the isotopically resolved rotational lines of the 1–0 band of this system. As a result, spectral simulations of the 0–0 band were repeated with the band origins of the $^{63,65}Cu_2$ and $^{65}Cu_2$ species treated as adjustable parameters. Very good agreement was obtained between simulation and experimental data as shown by trace (b) in Fig. 1 when shifts of $+0.06 \pm 0.02$ and $+0.12 \pm 0.04\ cm^{-1}$ were used for the $^{63,65}Cu_2$ and $^{65}Cu_2$ species, respectively. This approach was also used for simulation of the 0–0 band of the *B*–*X* system, with similar results [see trace (b) in Fig. 3]. In the remainder of this section we consider the sources of such electronic isotope shifts, and suggest that they contain useful information about the electronic structure of the *A* and *B* states of Cu_2.

TABLE IV. Observed and calculated line positions in (cm^{-1}) for the three isotopic forms of Cu_2 in 2–0 band of the *A*–*X* system.

Species	Assignment	Experimental	Calculated	Difference
$^{63}Cu_2$	*R*(4)	20 779.682	20 779.667	−0.015
	R(3)	20 779.542	20 779.530	−0.012
	R(2)	20 779.383	20 779.377	−0.005
	R(1)	20 779.232	20 779.208	−0.024
	R(0)	20 779.042	20 779.023	−0.019
	P(1)	20 778.572	20 778.605	+0.033
	P(2)	20 778.362	20 778.372	+0.010
	P(3)	20 778.142	20 778.123	−0.019
	P(4)	20 777.862	20 777.859	−0.003
	P(5)	20 777.522	20 777.578	+0.056
	P(6)	20 777.282	20 777.282	+0.000
$^{63}Cu^{65}Cu$	*R*(4)	20 776.962	20 777.004	+0.042
	R(3)	20 776.812	20 776.869	+0.057
	R(2)	20 776.702	20 776.718	+0.016
	R(1)	20 776.532	20 776.551	+0.019
	R(0)	20 776.312	20 776.369	+0.057
	P(1)	20 775.912	20 775.957	+0.045
	P(2)	20 775.692	20 775.728	+0.036
	P(3)	20 775.412	20 775.483	+0.071
	P(4)	20 775.172	20 775.223	+0.051
	P(5)	20 774.892	20 774.947	+0.055
	P(6)	20 774.582	20 774.655	+0.073
$^{65}Cu_2$	*R*(4)	20 774.242	20 774.317	+0.075
	R(3)	20 774.112	20 774.186	+0.074
	R(2)	20 773.962	20 774.037	+0.075
	R(1)	20 773.802	20 773.873	+0.071
	R(0)	20 773.622	20 773.694	+0.072
	P(1)	20 773.182	20 773.289	+0.107
	P(2)	20 773.002	20 773.063	+0.061
	P(3)	20 772.752	20 772.822	+0.070
	P(4)	20 772.472	20 772.566	+0.094
	P(5)	20 772.222	20 772.294	+0.072
	P(6)	20 771.912	20 772.007	+0.095

B. Electronic isotopic shifts

A theory of mass-related isotope shifts in the spectroscopy of molecular species has been presented by Bunker[25,26] and Watson.[27,28] Their treatments involve consideration of breakdown in the Born–Oppenheimer approximation, which is addressed by retaining the dependence of the electronic wave function on the nuclear kinetic energy operator. Estimates of the magnitude of the electronic isotope shifts $\Delta\nu_e$ can be obtained in the adiabatic approximation for pure Hund's case (a) Σ states, α and β, by using the van Vleck[27–29] expression:

$$\Delta\nu_e = [B_e - B_e^i]^\alpha \langle \hat{L}^2 \rangle^\alpha - [B_e - B_e^i]^\beta \langle \hat{L}^2 \rangle^\beta. \quad (8)$$

In this expression B_e and B_e^i are the equilibrium rotational constants of the lighter and heavier isotopic combinations, respectively, while the superscripts α and β denote the two electronic states involved in a given transition. The expectation value of the square of the orbital angular momenta $\langle \hat{L}^2 \rangle$ for the states α and β can be approximated by evaluating their separated atom values. To utilize this approach, it is

necessary to identify the atomic asymptotes of the two molecular states at their dissociation limits. For the $X\,^1\Sigma_g^+$ state of Cu_2 this is clearly the $^2S + {}^2S$ combination, while for the excited *A* and *B* $^1\Sigma_u^+$ states it is most likely the $^2D + {}^2S$ combination. Using these atomic states with $l_a = 2$ and $l_b = 0$ in the expression

$$\langle \hat{L}^2 \rangle = [l_a(l_a + 1) + l_b(l_b + 1)], \tag{9}$$

gives $\langle \hat{L}^2 \rangle = 6$ for the *A* and *B* excited states of Cu_2 and $\langle \hat{L}^2 \rangle = 0$ for the ground state.

The measured isotope shift between $^{63}Cu_2$ and $^{63}Cu^{65}Cu$ for the 0–0 band of the *B*–*X* transition is $\sim -0.02\ cm^{-1}$ while the value predicted by Eq. (5) is $-0.08\ cm^{-1}$, resulting in an electronic isotope shift of $+0.06\ cm^{-1}$. Evaluating the electronic isotope shift in terms of Eq. (8) and the spectroscopic constants given in Table III, a small shift of $+0.009\ cm^{-1}$ is predicted for both the *A*–*X* and *B*–*X* transitions. The signs of the shifts are correct in that they result in the line positions of the heavier combination being shifted to lower energy (see Appendix A for sign convention). However, their magnitude is significantly smaller than what is required to account for the observed electronic isotope shifts. It should be mentioned that if the excited *A* and *B* states of Cu_2 are considered to have a $Cu(^2D) + Cu(^2D)$ asymptote, the correction due to Eq. (8) is double the value calculated using a $Cu(^2D) + Cu(^2S)$ asymptote but still significantly less than what is observed. Because of the inherent assumptions in the approximate expression [Eq. (8)] used to describe the electronic isotope shift, it is perhaps not surprising that the agreement is poor. At present no high-level electronic structure calculations appear to exist for the excited states of Cu_2, so a more refined treatment is not possible.

A final possible origin of an isotope shift arises when describing an electronic state potential with Dunham coefficients.[24] The Y_{00} term is nonzero if a potential is not well described by a Morse function and is given explicitly as

$$Y_{00} = \frac{B_e - \omega_e x_e}{4} + \frac{\alpha_e \omega_e}{12 B_e} + \left(\frac{\alpha_e \omega_e}{12 B_e}\right)^2 \frac{1}{B_e}. \tag{10}$$

Using the *X* state spectroscopic constants in Table III a value of Y_{00} close to zero is obtained. Values calculated with the *A* and *B* excited state spectroscopic constants are larger by an order of magnitude than that obtained for the ground state. However, the isotopic variation in these values is very small, and Y_{00} will therefore not contribute significantly to an isotope shift.

C. Atomic isotope shifts

Because of the lack of information in the literature regarding electronic isotope shifts in molecular systems, it is difficult to rationalize the relatively large shift observed in this study for the moderately heavy diatomic species Cu_2. In contrast to the sparsity of information regarding such effects in molecular systems, isotope shifts in the optical spectra of atomic species have been studied in great detail for several decades since these shifts often yield valuable information pertaining to nuclear structure.[3,30–34] In the following section, the origins of atomic isotope shifts in optical spectroscopy will be presented, and the factors contributing to the shifts in the lowest levels of atomic copper will be discussed in particular.

The phenomenon of isotope shifts in atomic systems is related to a combination of two factors whose relative contributions depend on the mass of the species under consideration. For the elements of low atomic mass, isotopic variation corresponds to significant differences in the electron/nuclear-reduced masses and thereby leads to characteristic isotope shifts. Heavier elements on the other hand do not have appreciable differences in the electron/nuclear reduced masses but instead show significant differences in the charge distribution in their extended nuclear volumes. The former effect, called the *mass shift*, dominates for the elements early in the periodic table, while for the heavier elements the *field shift* or *volume effect* is the most significant origin of isotopic shifts. For the intermediate elements a combination of the two factors can exist. Rigorously, the mass shift described thus far is valid for single electron hydrogenic atomic systems only, while for all others another mass-related term exists. The additional term arises from the coupling of angular momenta between the electrons and is therefore state specific. By convention, this latter mass-related shift is called the *specific mass shift*, while the former is called the *normal mass shift*.[35]

Isotopic shifts in the optical spectra of the low-lying levels of atomic copper generated in cooled discharges have been examined interferometrically[36–38] and more recently with high-resolution laser optogalvanic[39] and fluorescence[40] spectroscopies. Spectra recorded in the present study for the $^2P_{1/2}$–$^2D_{3/2}$ transition at 5782 Å are shown in Fig. 5. Signals were recorded by scanning the dye laser through the 5782 Å transition while monitoring the ultraviolet fluorescence of the more strongly allowed $^2P_{1/2}$–$^2S_{1/2}$ radiative decay channel at 3274 Å. The observed structure arises from the magnetic hyperfine interaction present in the *P* and *D* states, the electric quadrupole interaction in the $^2D_{3/2}$ level and the duplication of these splittings due to the isotope shift between ^{63}Cu and ^{65}Cu. For a given isotope the hyperfine splitting of a level can be represented by the zero-field expression[30] as

$$\Delta E_F = \frac{AC}{2} + BC(C + 1), \tag{11}$$

where $C = F(F + 1) - J(J + 1) - I(I + 1)$, *J* is the total electronic angular momentum, *I* is the nuclear spin angular momentum, and *F* is the total atomic angular momentum. *A* and *B* are the magnetic hyperfine and electric quadrupole interaction terms, respectively. The first term in this expression is the magnetic hyperfine splitting, while the second describes the deviation from the regular Landé splitting interval resulting from the electric quadrupole interaction. Line intensities can be obtained by assuming a statistical population distribution in the ground level and by assigning statistical weight factors to the values of *F* coupled in a radiative transition. Tabulations of such intensity factors are given in Kopfermann[30] and Kuhn.[3] With the line positions and intensities, simulated spectra for the $^2P_{1/2}$–$^2D_{3/2}$ transition were generated by convoluting with a Gaussian line shape function representing the laser linewidth.

With the present $0.07\ cm^{-1}$ spectral resolution of the

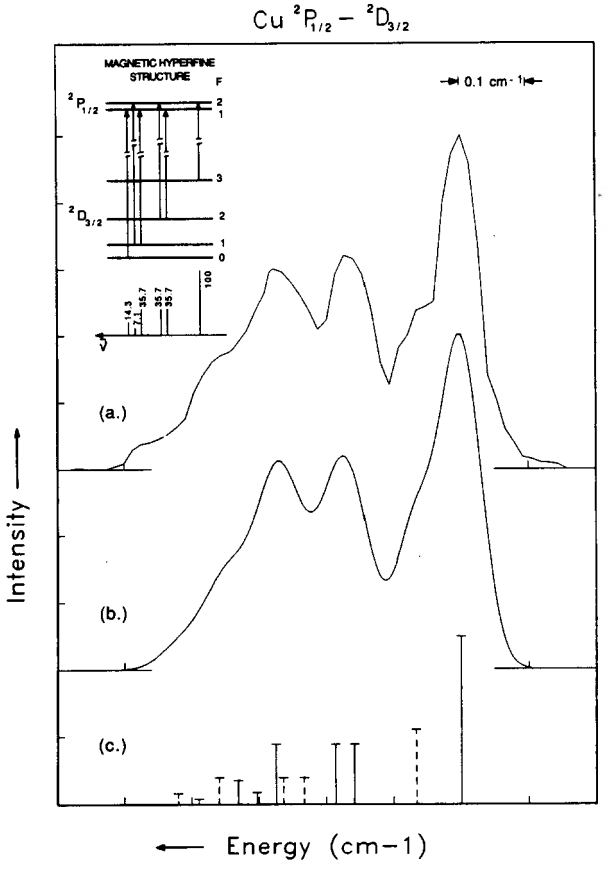

FIG. 5. Magnetic hyperfine and isotope structure on the observed [trace (a)] and simulated [trace (b)] spectra of the $3d^{10}4p^1\,{}^2P_{1/2} \leftarrow 3d^9 4s^2\,{}^2D_{3/2}$ copper atom transition at 5872 Å. Inset shows a schematic representation of the predicted line positions and their relative intensities arising from the allowed zero-field transitions ($\Delta F = 0 \pm 1$) amongst the magnetic hyperfine levels (F) in the two states optically coupled for a single isotope of copper. The effect of electric quadrupole coupling in the $^2D_{3/2}$ levels is too small to be shown on this scale. Trace (c) shows the relative line positions and intensities of the six hyperfine transitions possible between $^2P_{1/2}$ and $^2D_{3/2}$ for both isotopic species of atomic copper. ^{63}Cu is represented by a solid line, ^{65}Cu by the dashed lines. The isotope shift of $+0.067$ cm^{-1} between the ^{63}Cu and ^{65}Cu species can be identified most readily on the right of this figure as the splitting between the $F = 2 \leftarrow F = 3$ hyperfine transitions of the two isotopes. With a spectral width (FWHM) of 0.07 cm^{-1} in the region of 5800 Å with the dye laser used, this splitting is only partially resolved on the right of trace (a).

Lumonics dye laser in the region of 5800 Å, the isotope shift in the $^2P_{1/2}$–$^2D_{3/2}$ transition is manifested as the partially resolved splitting on the extreme right of Trace (a) in Fig. 5. Best agreement between simulated and experimental spectra was obtained with an isotope shift of $+0.07 \pm 0.01$ cm^{-1} (see the Appendix for sign conventions). This value is in agreement with several higher resolution studies of this transition.[36–40] Isotope shifts of a similar magnitude were also observed in the transition involving the $^2D_{5/2}$ level, but isotope splittings in the ^2P_J–$^2S_{1/2}$ transitions were not resolved in the present study. This observation is in agreement with earlier measurements[36–40] where much smaller isotope shifts were observed in transitions between configurations not involving a change in the number of d electrons, i.e., ^2D states. In the terminology of atomic spectroscopy the anomalously large isotope shifts involving the ^2D states arise from the *specific mass shift*.[35,41]

From the similar magnitude and direction (see the Appendix) of the isotope shift in the lowest ^2D levels of atomic copper and the A–X, B–X transitions of Cu_2, it is desirable to correlate the isotope shift in the atomic and molecular systems. In other words, the molecular isotope shift appears to be a direct manifestation of the amount of atomic "d-hole" character in the bonding of the A and B states of Cu_2 versus that in the ground state.

D. Electronic structure of Cu_2

The low-energy molecular states of copper dimer are expected to arise from the following atomic copper asymptotes: $^2S_{1/2} + {}^2S_{1/2}$, $^2S_{1/2} + {}^2D_J$, $^2D_J + {}^2D_J$, and $^2S_{1/2} + {}^2P_J$. Numerous experimental studies[8,9,11,13–17] and recent *ab initio* calculations[19–21] indicate a large well depth for the $X\,{}^1\Sigma_g^+$ state of Cu_2. Thus, the ground state of Cu_2, like the alkali metal dimers, arises from the $^2S_{1/2} + {}^2S_{1/2}$ combination, giving rise to a $3d^{10}_{Cu}\,3d^{10}_{Cu}\,(4s\sigma)^2(4s\sigma^*)^0$ molecular orbital configuration. This assignment is bolstered by Bondybey's observation,[17] in the luminescence spectra of solid neon matrices containing molecular copper, of the corresponding molecular triplet state sharing the $^2S_{1/2} + {}^2S_{1/2}$ asymptote but having a $3d^{10}_{Cu}\,3d^{10}_{Cu}\,(4s\sigma)^1(4s\sigma^*)^1$ configuration.

In contrast to the electronic structure of the alkali metal dimers, the presence of a low-lying $3d^9 4s^2$ configuration in atomic copper significantly increases the number of possible low-lying molecular states of copper dimer. From the lowest energy $^2S + {}^2D$ asymptote a total of 12 molecular Hund's case (a) or (b) states are obtained with Λ,S coupling. They are spin singlets and triplets of Σ^+, Π, and Δ symmetry, each with odd and even parity combinations. Of these the $^1\Sigma_u^+$ and $^1\Pi_u$ states are significant in electric dipole radiative transitions to the $^1\Sigma_g^+$ ground state. Since both the A and B states of Cu_2 have been identified in the present study as $^1\Sigma_u^+$ [Hund's case (a)] some higher energy asymptotes must be considered to obtain a second state of this symmetry since only a single such state is obtained from the $^2S + {}^2D$ asymptote under strict Λ,S coupling. The next-higher energy asymptote is the $^2D + {}^2D$ pair, but restrictions imposed by the Pauli Exclusion Principle preclude certain combinations between identical states of a homonuclear molecule. As a result no transitions involving $\Delta\Lambda = 0$ can radiatively couple to the $^1\Sigma_g^+$ ground state from the molecular states derived from the $^2D + {}^2D$ asymptote. The $^2S + {}^2P$ asymptote at approximately 30 600 cm^{-1} [2] above the ground-state asymptote provides the requisite $^1\Sigma_u^+$ state, since this separated atom limit leads to $^1\Sigma_g^+$, $^1\Sigma_u^+$, $^3\Sigma_g^+$, $^3\Sigma_u^+$, $^1\Pi_g$, $^1\Pi_u$, $^3\Pi_g$, and $^3\Pi_u$ molecular states. It seems unlikely, however, that such a $^1\Sigma_u^+$ state would be bound by almost 26 000 cm^{-1}, which would be required to explain the existence of two low-lying $^1\Sigma_u^+$ states (A and B).

An approach that rationalizes the presence of two low-lying 0_u^+ states in Cu_2 is to treat the molecular bonding for the low-lying states of copper dimer in Hund's case (c). This coupling scheme is particularly appropriate for the molecular states derived from the copper atom $3d^9 4s^2$ configuration since the splitting between the desired $^2D_{3/2}$, $^2D_{5/2}$ atomic

spin–orbit levels is large, having a value of approximately 2043 cm^{-1}. The relation

$$\zeta(3d) = 2/5\Delta|E\,^2D_{3/2} - E\,^2D_{5/2}|,$$

gives the spin–orbit coupling constant $\zeta(3d)$ in the $3d^9 4s^2$ configuration as 817 cm^{-1}. Because of the large spin–orbit coupling constant in the ^2D state, it can be argued that the behavior of molecular states of Cu_2 having this asymptote, at least for large values of internuclear separation, are best described by the mutual coupling of the total angular momenta of the constituent atoms of Hund's case (c).

Coupling between $J_1 = 5/2$ and $J_2 = 1/2$ of the lowest energy asymptote $^2D_{5/2} + {}^2S_{1/2}$, yields 14 molecular states with Ω values of 3, 2, 2, 1, 1, 0^+, and 0^- each having *g* and *u* combinations. For an electric dipole transition coupling these molecular states to the 0_g^+ ground state, the only allowed selections of the 14 possibilities are two 1_u states and a single 0_u^+ state. The next higher energy asymptote involves the $^2D_{3/2} + {}^2S_{1/2}$ combination. Coupling between the total angular momenta $J_1 = 3/2$ and $J_2 = 1/2$ yields three molecular states 1_u $(x2)$ and 0_u^+, which can radiatively couple to the ground state. Thus, if *J,J* coupling is considered in the separated atom limit, the origin of the closely lying A and B 0_u^+ states of Cu_2 can be obtained directly from the $^2D_{5/2} + {}^2S_{1/2}$ and $^2D_{3/2} + {}^2S_{1/2}$ asymptotes. Approximate potential curves dissociating to these limits, based on the values of ω_e and T_e, are depicted in Fig. 6.

Several molecular states are obtained by considering the $^2D_J + {}^2D_J$ asymptote at approximately double the energy of the $^2D_J + {}^2S_{1/2}$ asymptotes. However, only the $^2D_{3/2} + {}^2D_{5/2}$ combination produces a state that can radiatively couple to the 0_g^+ ground state with $\Delta\Omega = 0$. Two 0_u^+ states result from the $^2D_{3/2} + {}^2D_{5/2}$ asymptote whereas no such states are obtained from the $^2D_{5/2} + {}^2D_{5/2}$ and $^2D_{3/2} + {}^2D_{3/2}$ pairs due to combination restrictions when $J_1 = J_2$. As with the $^2S_{1/2} + {}^2S_{1/2}$ asymptote of ground state Cu_2, Hund's case (c) treatment of the molecular states arising from the $^2P_J + {}^2S_{1/2}$ pair is inappropriate due to the small (~ 166 cm^{-1}) spin–orbit coupling constant $\zeta(4p)$ of the atomic $3d^{10}4p^1$ configuration. For generality, however, only the $^2P_{3/2} + {}^2S_{1/2}$ asymptote will result in a single 0_u^+ molecular state that can radiatively couple to the 0_g^+ ground state.

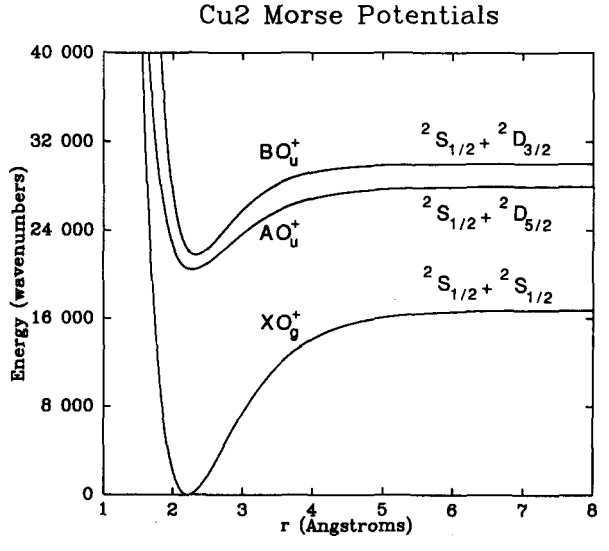

FIG. 6. Curves derived from a Hunds case (c) description of the low-energy molecular states of Cu_2 by considering the $^2S_{1/2} + {}^2S_{1/2}$ and $^2D_J + {}^2S_{1/2}$ asymptotes. The curves shown are Morse potentials obtained using the vibrational constants ω_e and the internuclear separations r_e, which were obtained from the rotational constants listed in Table III. Well depths were calculated using the observed T_e values and by selecting the atomic asymptotes sequentially closest in energy to the *A* and *B* states.

As mentioned previously the magnitude of the spin–orbit coupling constant $\zeta(3d)$ for the $3d^9 4s^2$ configuration of atomic copper indicates that an appropriate description of the molecular states derived from asymptotes having the $3d^9 4s^2$ configuration lies in Hund's case (c) rather than cases (a) or (b). It can be concluded from the foregoing discussion that if the low-lying optically accessible molecular states of Cu_2 are treated in case (c) coupling, the A and B states should both have a dominant atomic "*d*-hole" configuration. This provides a rationalization of the previously presented correlation between the large isotope shift associated with the ^2D levels ($3d^9 4s^2$ configuration) of atomic copper and the anomalously large electronic isotope shifts measured in the present study of the A and B states of copper dimer. Further development of this idea awaits the availability of refined *ab initio* calculations of the excited states in Cu_2 that incorporate relativistic effects such as spin-orbit coupling.

E. Dynamical effects

Another consequence of the *J–J* coupling scheme is that the density of nondegenerate electronic states increases dramatically from that obtained under the $\Lambda\Sigma$ coupling scheme. Thus, while the task of identifying asymptotes for the 0_u^+ excited states, which can radiatively couple to the ground state with $\Delta\Omega = 0$ is, as previously shown, rather straightforward, that of identifying asymptotes for transitions involving $\Delta\Omega > 0$ is more daunting. Associated with this high density of electronic states is the expectation of numerous spectroscopic perturbations and dynamical effects among these excited states. Radiative lifetime measurements of Bondybey[13] in an effusive source for the first few vibrational levels of the *A* state of Cu_2 showed pressure-independent variations indicative of increasing predissociation rates in higher levels. Likewise, by examining the decay kinetics in a study of the pressure-dependent radiative lifetimes of the *B* and *B'* (also labeled *C*[5]) states Bondybey demonstrated collisional equilibration of population between these two states.[13]

Corroborative evidence of pronounced dynamical effects in the spectroscopy of the *A* and *B* states of Cu_2 can be found in several matrix-isolation absorption and laser excitation studies. Reported spectra indicate completely featureless profiles for the absorption processes from the ground state. In contrast, dispersed emission spectra show vibrationally relaxed emission to the ground state, with well-resolved vibrational progressions whose splittings are comparable with the gas phase values.[15–18] It is likely that the structureless excitation spectra and vibrationally relaxed emission observed in these systems arise from phonon-assist-

ed irreversible energy migration in the solid among the dense set of electronic states present in the vicinity of the optically accessible *A* and *B* states.

The dynamical implications of such relaxation processes are quite interesting. For example, they provide an explanation of the discrepancies reported by Bondybey[16] between experimental and calculated Franck–Condon factors for the 0–0 bands in the vibrationally relaxed $A \rightarrow X$ and $B \rightarrow X$ systems, where good agreement exists for the remaining $0' \rightarrow v''$ bands. It can be argued that under solid state conditions complete vibrational relaxation in the upper electronic states results in no spectral overlap between absorption and emission bands with the exception of the transitions between the vibrationless levels, i.e., 0′–0″. If account is taken of reabsorption effects on the 0′–0″ bands of the *A*–*X* and *B*–*X* systems of copper dimer in a solid with a high number density of optically active species, good agreement exists between experimental and calculated spectra for all the vibrational transitions. A further dynamical effect is the observation of the long-lived $^3\Sigma_u^+$ state of Cu_2 in solid neon samples explained by Bondybey as arising from the cage-induced recombination of incompletely dissociated atomic species produced via efficient excited state predissociation events.[17]

VI. CONCLUSIONS

Laser-induced fluorescence excitation spectra recorded in the present study for the *A*–*X* and *B*–*X* systems of Cu_2 demonstrate conclusively that the *A* and *B* states are of $^1\Sigma_u^+$ [or 0_u^+, Hund's case (c) notation] symmetry. Spectral simulations indicate anomalous isotope shifts for both the *A*–*X* and *B*–*X* systems. Consideration of the differences in vibrational and rotational constants between the three isotopic variants of molecular copper dimer show these to be insufficient to account for the observed shifts. It is therefore concluded that pronounced electronic isotope shifts are present in the *A* and *B* states, and are approximately equal in the two states. Comparison of the magnitude and sign of the observed molecular isotope shifts with the large specific mass shift in the ^2D spin–orbit levels of atomic copper (derived from the $3d^9 4s^2$ configuration) indicates strong correlation between the two phenomena. In view of this observation, a *J*,*J* coupling scheme is presented for the low-energy $^2D_J + {}^2S_{1/2}$ asymptotes of copper dimer. Considering coupling between the total angular momenta in the $^2D_{5/2} + {}^2S_{1/2}$ and $^2D_{3/2} + {}^2S_{1/2}$ asymptotes in Hund's case (c), two molecular states of 0_u^+ symmetry are obtained. This scheme predicts equal amounts of the $3d^9 4s^2$ atomic like configuration in the *A* and *B* molecular 0_u^+ states and is therefore in agreement with the observation of large and identical isotope shifts in these states. Hund's case (c) coupling in the excited states of Cu_2 results in dynamical effects including predissociation of the *A* state under low-pressure gas phase conditions and efficient vibrational relaxation of the *A* and *B* states in solid neon matrices.

In spite of the success obtained by treating the molecular bonding in the low-energy-excited states of Cu_2 in Hund's case (c), some peculiarities still exist. For example, the vibrational frequency of the *A* state is considerably less than the *B* state, 192 and 245 cm^{-1}, respectively, while the equilibrium bond lengths for these two states are opposite to what is predicted by the much used Badger's rule[42] of $r_e^2 \propto \omega_e^{-1}$, i.e., the bond length of the latter is greater than the former, 2.28 and 2.38 Å, respectively. These characteristics may indicate some nonadiabatic behavior in the molecular potentials derived from *J*,*J* coupling in the separated atom limits or subtleties associated with copper dimer bonding between $^2S_{1/2} + {}^2D_J$ atoms in the two spin–orbit levels.

Yet another peculiarity exhibited by the *A* and *B* states of Cu_2 is related to their short radiative lifetimes. Measurement of the radiative lifetimes repeated[43] in the present study were found to agree approximately with those of Bondybey,[13] who obtained intrinsic radiative lifetimes for the *A* and *B* states as 115 ± 10 and 40 ± 5 ns, respectively. Thus, if, as proposed, the molecular bonding in these two states arises from the $^2S_{1/2} + {}^2D_J$ atomic copper asymptotes it would be expected[44] that the resulting molecular states would show a small oscillator strength corresponding to the forbidden atomic ^2D–^2S transition. However, small admixtures of configurations arising from the very short lived $3d^{10}4p^1\ {}^2P_J$ atomic state[45] in the *A* and *B* states could induce a significant oscillator strength in the molecular electric dipole transition to the ground state.

It is rather evident from the foregoing remarks that there is a great need for high-level *ab initio* calculations of the excited states of Cu_2 incorporating relativistic effects like spin-orbit coupling. Experimentally, a study of the electric quadrupole hyperfine structure on the rotational lines in the *A*–*X* and *B*–*X* systems of Cu_2 would assist greatly in determining in extent of atomic *d*-orbital contributions in the *A* and *B* states. The spectral resolution required in such a study would be < 0.01 cm^{-1}, because as mentioned in the simulation section, an inspection of individual rotational transition line shapes recorded with the 0.08 cm^{-1} resolution of the present study indicated featureless profiles.

After this paper was submitted, we were made aware of a study of the Cu_2 (*A*–*X*) and Cu_2 (*B*–*X*) transitions using the technique of mass-resolved laser photoionization spectroscopy, the results of which[46] confirm our assignment of the *A* state as well as the magnitudes of the isotope shifts observed for the *A* and *B* states. These studies[46] demonstrate electronic isotope shifts of 0.068 and 0.063 cm^{-1} for the *A*–*X* 0–0 and *B*–*X* 0–0 bands, respectively, for the $^{63}Cu^{65}Cu$ isotope, with respect to the $^{63}Cu_2$ species. Within the error limits of the measurements, these results are in agreement with those reported here.

ACKNOWLEDGMENTS

We gratefully acknowledge support of this research by the National Science Foundation, Grants Nos. CHE-86-03613 (WHB) and CHE-85-21050 (MDM). Acknowledgment is also made to the Donors of the Petroleum Research Fund, administered by the American Chemical Society, for partial support of this research.

APPENDIX

The sign conventions adopted in the study of atomic electronic isotope shifts and for molecular rotational and

vibrational isotope shifts are opposite, so care is necessary when comparing contributions from both effects. According to Eq. (5), a vibrational isotope shift in molecular systems is defined as positive when the transition of the smaller mass combination occurs at a higher energy than that of the larger mass combination. In contrast, an electronic isotope shift on an atomic transition is defined as positive if the isotope of greater mass is observed at higher energy. The latter convention can be rationalized for hydrogenic systems using the following arguments.

Assuming infinite nuclear mass, the energy T_∞ of a given level is proportional to the term value n of that level. Explicitly, T_∞ is given as

$$T_\infty = R_\infty Z^2/n^2, \tag{A1}$$

where Z is the nuclear charge and R_∞ is the Rydberg constant for a nucleus of infinite mass. By incorporating a finite atomic mass M, the so-called "Bohr correction" is made to the term value, viz.,

$$T = T_\infty (1 - m/M),$$

with m the electron mass. Thus, the term energy T of an isotope of greater mass M_2 is displaced less from a series limit T_∞ than the isotope of lesser mass M_1. In a given level, the term energy difference ΔT between the two isotopes is therefore:

$$\Delta T = m\left(\frac{1}{M_1} - \frac{1}{M_2}\right) T_\infty . \tag{A2}$$

For a transition involving two terms whose principal quantum numbers are $n_2 > n_1$, the observed transition energy of the heavier isotope occurs at higher energy than the lighter one because of the larger displacement in term energy of the lower level n_1 [see Eq. (A1) and (A2)]. A generalized scheme of this behavior is depicted in the left side of Fig. 7 for three levels, n_3, n_2, and n_1. It is evident from this figure that the transition energy of the heavier isotope (shown by dashed lines) will always be greater than that of the lighter one (shown by solid lines) regardless of which levels n_3, n_2, or n_1 are involved in the optical transition. Elements of low atomic mass follow this behavior of *normal mass shifts*, but in multielectron systems, another coupling is possible by virtue of a more complicated transformation to the center of mass frame, which results in effective two body interactions. This coupling is called the *specific mass shift* and the relative signs are not predictable, since they can vary with electronic configuration. Furthermore, depending on whether the specific mass shift exists in the lower or upper level in a transition, the sign can be positive or negative.

Shown schematically on the right of Fig. 7 are the isotope shifts present in the lowest energy electronic configurations of atomic copper. In the $3d^{10}4p\ ^2P_{1/2}$–$3d^9 4s^2\ ^2D_{3/2}$ transition of atomic copper the observed sign of the shift is positive (i.e., $\nu\ Cu^{65} > \nu\ Cu^{63}$). Transitions coupling to the $^2D_{3/2}$ level but originating in the ground $^2S_{1/2}$ would, if observed, show a negative isotope shift. Taking into account the reversed sign convention adopted in atomic and molecular systems for the study of isotope shifts, transitions between states having the aforementioned atomic asymptotes would therefore exhibit a positive isotope shift in the molecular convention. The inferred shift to lower energy on the atomic transition of ^{65}Cu is therefore of the correct magnitude and direction to explain the anomalously large electornic isotope shift observed on the *A*–*X* and *B*–*X* systems of copper dimer.

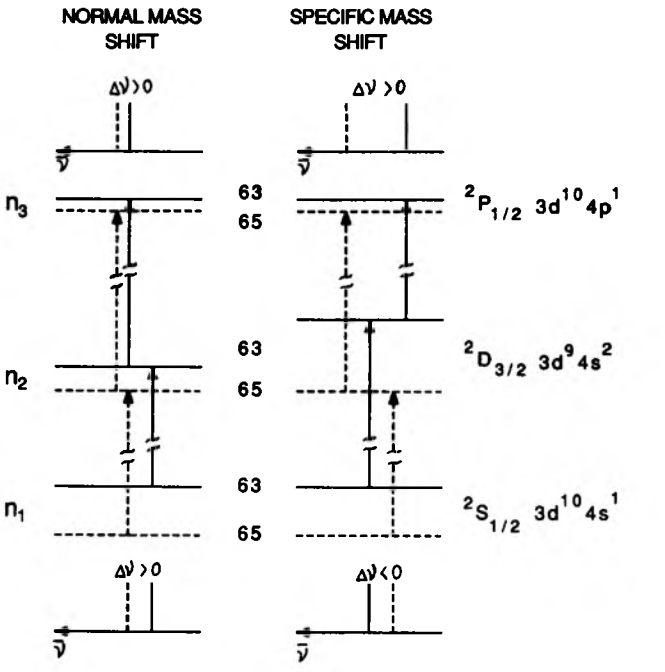

FIG. 7. Schematic representation of the normal and specific mass shifts present in the optical spectroscopy of atomic systems. The left of this figure depicts the normal mass shift for two isotopes in two transitions between the levels n_3, n_2, and n_1. Note that the transition for the species of greater atomic mass (shown by dashed lines) occurs at higher frequency. The configuration dependent isotope shifts for the three lowest configurations of atomic copper are shown on the right of this figure. A large specific mass shift in the $3d^9 4s^2$ configuration results in the observed positive isotope shift in the $^2P_{1/2}$–$^2D_{3/2}$ transition. By inference, this specific mass shift produces a negative atomic isotope shift in the forbidden $^2D_{3/2}$–$^2S_{1/2}$ transition.

[1]W. H. Breckenridge, in *Reactions of Small Transient Species*, edited by A. Fontijn and M. A. A. Clyne (Academic, New York, 1983); W. H. Breckenridge, Acc. Chem. Res. **22**, 21 (1989).
[2]C. E. Moore, Natl. Stand. Ref. Data Ser. Natl. Bur. Stand. 35, (U. S. GPO, Washington, D. C., 1971), Vol. I–III.
[3]H. G. Kuhn, *Atomic Spectra*, 2nd ed. (Longmans, London, 1970).
[4]K. P. Huber and G. Herzberg, *Molecular Spectra and Molecular Structure IV. Constants of Diatomic Molecules* (Von Nostrand Reinhold, New York, 1979).
[5]M. D. Morse, Chem. Rev. **86**, 1049 (1986).
[6]M. E. Geusic, M. D. Morse, S. C. O'Brien, and R. E. Smalley, Rev. Sci. Instrum. **56**, 2123 (1985).
[7]R. E. Smalley, L. Wharton, and D. H. Levy, Acc. Chem. Res. **10**, 139 (1977).
[8]B. Kleman and S. Lindkvist, Ark. Fys. **8**, 333 (1954).
[9]N. Åslund, R. F. Barrow, W. G. Richards, and D. N. Travis, Ark. Fys. **30**, 171 (1965).
[10]D. S. Pesič and S. Weniger, C. R. Hebd. Seances Acad. Sci. Ser. B **273**, 602 (1971).
[11]J. Lochet, J. Phys. B **11**, L55 (1978).
[12]D. R. Preuss, S. A. Pace, and J. L. Gole, J. Chem. Phys. **71**, 3553 (1979).
[13]V. E. Bondybey, G. P. Schwartz, and J. H. English, J. Chem. Phys. **78**, 11 (1983).
[14]E. A. Rohlfing and J. J. Valentini, J. Chem. Phys. **84**, 6560 (1986).
[15]J. L. Gole, J. H. English, and V. E. Bondybey, J. Phys. Chem. **86**, 2560 (1982).
[16]V. E. Bondybey and J. H. English, J. Phys. Chem. **87**, 4647 (1983).

[17]V. E. Bondybey, J. Chem. Phys. **77**, 3771 (1982).
[18]H. Wiggenhauser, D. M. Kolb, H. H. Rotermund, W. Schrittenlacher, and W. Schroeder, Chem. Phys. Lett. **122**, 71 (1985).
[19]K. Raghavachari, K. K. Sunil, and K. D. Jordan, J. Chem. Phys. **83**, 4633 (1985).
[20]R. L. Martin, J. Chem. Phys. **78**, 5840 (1983); H.-J. Werner and R. L. Martin, Chem. Phys. Lett. **113**, 451 (1985).
[21]M. Witko and H.-O. Beckmann, Mol. Phys. **47**, 945 (1982).
[22]R. R. Bennett, J. G. McCaffrey, I. Wallace, D. J. Funk, A. Kowalski, and W. H. Breckenridge, J. Chem. Phys. **90**, 2131 (1989).
[23]G. Herzberg, *Spectra of Diatomic Molecules* (Van Nostrand Reinhold, New York, 1950).
[24]H. Lefebvre-Brion and R. W. Field, *Perturbations in the Spectra of Diatomic Molecules* (Academic, Orlando, Florida, 1986).
[25]P. R. Bunker, J. Mol. Spectrosc. **28**, 422 (1968).
[26]P. R. Bunker, J. Mol. Spectrosc. **42**, 478 (1972); *ibid.* **45**, 151 (1973).
[27]J. K. G. Watson, J. Mol. Spectrosc. **45**, 99 (1973).
[28]J. K. G. Watson, J. Mol. Spectrosc. **80**, 411 (1980).
[29]J. H. Van Vleck, J. Chem. Phys. **4**, 327 (1936).
[30]H. Kopfermann, *Nuclear Moments* (Academic, New York, 1958).
[31]A. Steudel, in *Hyperfine Interactions*, edited by A. J. Freeman and R. B. Frankel (Academic, New York, 1967).
[32]D. N. Stacey, Rep. Prog. Phys. **29**, 171 (1966).
[33]J. Bauche and R.-J. Champeau, Adv. At. Mol. Phys. **12**, 39 (1976).
[34]W. H. King, *Isotope Shifts in Atomic Spectra* (Plenum, New York, 1984).
[35]D. S. Hughes and C. Eckart, Phys. Rev. **36**, 694 (1930).
[36]S. Wagner, Z. Phys. **141**, 122 (1955).
[37]K. Murakawa, J. Phys. Soc. Jpn. **11**, 774 (1956).
[38]W. Fischer, Z. Phys. **161**, 89 (1961).
[39]D. C. Gerstenberger, E. L. Latush, and G. J. Collins, Opt. Commun. **31**, 28 (1979).
[40]Ph. Dabkiewicz and T. W. Hansch, Opt. Commun. **38**, 351 (1981).
[41]Recently a reformulation of the theory of mass and field effects in atomic isotope shifts has been presented that addresses the validity of separating normal and specific mass shifts. For details see S. A. Blundell, P. E. G. Baird, C. P. Botham, C. W. P. Palmer, D. N. Stacey, and G. K. Woodgate, J. Phys. B **17**, 53 (1984); S. A. Blundell, P. E. G. Baird, C. W. P. Palmer, D. N. Stacey, and G. K. Woodgate, *ibid.* **20**, 3663 (1987); C. W. P. Palmer, *ibid.* **20**, 5987 (1987).
[42]R. M. Badger, J. Chem. Phys. **2**, 128 (1934); **3**, 710 (1935).
[43]R. R. Bennett, J. G. McCaffrey, and W. H. Breckenridge (unpublished).
[44]Z.-W. Fu and M. D. Morse, J. Chem. Phys. **90**, 3417 (1989).
[45]A. Bielski, J. Quant. Spectrosc. Radiat. Transfer **15**, 463 (1975).
[46]P. R. R. Langridge-Smith (private communication).